Finite Element Analysis of Tissue Conductivity during High-frequency and Low-voltage Irreversible Electroporation

Amir Khorasani[1], Seyed Mohammad Firoozabadi*[1], Zeinab Shankayi[1]

[1] Department of Medical Physics, School of Medical Sciences, Tarbiat Modares University, Tehran, Iran

A R T I C L E I N F O	A B S T R A C T
	Introduction: Irreversible electroporation (IRE) is a process in which the membrane of the cancer cells are irreversibly damaged with the use of high-intensity electric pulses, which in turn leads to cell death. The IRE is a non-thermal way to ablate the cancer cells. This process relies on the distribution of the electric field, which affects the pulse amplitude, width, and electrical conductivity of the tissues. The present study aimed to investigate the relationship of the pulse width and intensity with the conductivity changes during the IRE using simulation. *Materials and Methods:* For the purpose of the study, the COMSOL 5 software was utilized to predict the conductivity changes during the IRE. We used 4,000 bipolar and monopolar pulses with the frequency of 5 kHz and 1 Hz, width of 100 μs, and electric fields of low and high intensity. Subsequently, we built three-dimensional numerical models for the liver tissue. *Results:* The results of our study revealed that the conductivity of tissue increased during the application of electrical pulses. Additionally, the conductivity changes increased with the elevation of the electric field intensity. *Conclusion:* As the finding of this study indicated, the IRE with high-frequency and low electric field intensity could change the tissue conductivity. Therefore, the IRE was recommended to be applied with high frequency and low voltage.

Introduction

Electroporation is a physical transfection method in which the cell membrane permeability to ions and macromolecules is increased by the employment of short and high electric field pulses [1]. This process is caused by the creation of nanoscale pores in the cell membrane. The creation of the pores is dependent on the distribution of the electric field [2]. On the other hand, the electric field distribution and magnitude inside the target tissue rely on the electrical pulse parameters and tissue properties, such as electrical conductivity [3].

Miklavcic et al. demonstrated that sufficient electric field coverage is necessary for effective electroporation treatment [4]. Electroporation can either induce temporary or permanent pores and be referred to as reversible (RE) or irreversible electroporation (IRE), respectively [5]. The RE is used for the introduction and transfer of macromolecules, such as DNA and protein into the cells. The combined application of the RE with chemotherapy is called electrochemotherapy, which is employed in cancer treatment. This process can obtain complete response of entire body.

The IRE was developed to kill the cancer cells. We can use this ablation technique without triggering the entire body. The factors that affect the RE and IRE of the cells include electric field magnitude (voltage) and frequency as well as the period, duration, shape, and number of electric pulses [6]. The IRE pulses can be divided into two groups, including high-frequency/low-voltage and low-frequency/high-voltage.

The clinical application of the IRE with low-frequency is performed under general anesthesia to eliminate the patient's pain. Pain can be caused by muscle contractions during each low-frequency and high-voltage electrical pulse [7]. The threshold for nerve stimulation, which causes muscle contraction, increases as the pulse frequency is elevated [8]. The IRE with high frequency or low voltage eliminates the patient's pain during the clinical applications and produces lower temperature in the tissue [7, 9].

Regarding this, we utilized electric pulses with high frequency and low voltage. The uniformity of the electric field inside the tissue and sufficient electric filed magnitude are issues of fundamental significance [10]. The electrical conductivity of the tissue is an important factor, which affects the distribution of the electric field within the electroporated tissues.

Corresponding Author: Department of Medical Physics, School of Medical Sciences, Tarbiat Modares University, Tehran, Iran Tel: +98 21 82883821, Fax: +98 21 82883828, Email: pourmir@modares.ac.ir

Different studies have shown that an immediate increase in conductivity was caused by high-voltage and low-frequency pulses [11-13]. Conductivity changes are much higher in the IRE than that in the RE [14]. The measurement of tissue electrical properties (e.g., specific electrical conductivity) is proposed to optimize the efficiency of electroporation protocols [15-17]. With this background in mind, the present study was conducted to compare the conductivity changes during the high-frequency and low-voltage IRE with those in the low-frequency and high-voltage IRE.

Materials and Methods

Pulse features and geometry

In order to investigate the conductivity changes of the liver tissue during the IRE, we modeled a plate electrode. The plate electrodes were stainless steel with length of 20 mm, width of 6 mm, thickness of 0.5 mm, and electrode gaps of 4.4 mm. The liver as a three-dimensional rectangular object with dimensions of 20 mm width, 4.4 mm depth, and 20 mm height was simulated (Figure 1).

In the present study, mainly two different parameters of electric pulses were simulated, including low-voltage and high-frequency (LVHF) as well as high-voltage and low-frequency (HVLF) pulses. The LVHF protocols involved 4,000 bipolar and monopolar pulses with the frequency of 5 kHz, pulse width of 100 μs, and electric fields intensity of 100-300 V/cm with steps of 50 V/cm.

On the other hand, the HVLF protocols included 8 bipolar and monopolar pulses with the frequency of 1 Hz, pulse width of 2 ms, and electric field intensity of 2500 V/cm as a representative pulse sequence of classic IRE with low frequency. The electric conductivity of the liver was investigated for two candidate points, namely tip of the electrode and between the electrodes.
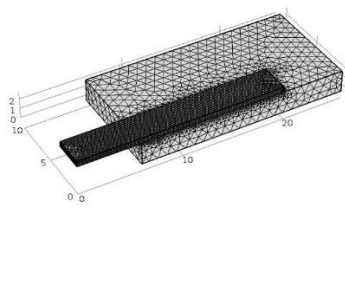

Figure 1. Geometry and mesh visualization of numerical modeling

Numerical model

The model was performed using the COMSOL Multiphysics software version 5.0 with a triangular mesh that contained 58,864 mesh nodes. The geometry of the electrode and tissue was built in a symmetric model in order to reduce the simulation time (Figure 1).

The electric field distribution inside the target tissue was calculated using the Laplace's equation

$$\vec{\nabla}.(\sigma \vec{\nabla}\varphi) = 0 \tag{1}$$

Where σ and φ are electrical conductivity and electrical potential, respectively. The electrical boundary condition at the active electrode was intended to be the electrical potential $\varphi = V_0$, and another electrode was not active to $\varphi = 0$. The tissue surfaces, which were not in contact with the electrode, were considered as electrical insulation. The temperature changes in the liver tissue were estimated using the Pennes Bioheat equation:

$$\nabla.(k\nabla T) + \sigma|\nabla\varphi|^2 + q''' - W_b c_b T = \rho c_p \frac{\partial T}{\partial t} \tag{2}$$

Where T is temperature, φ is electrical potential, q''' is the heat produced by metabolism, $W_b c_b T$ is the heat produced by perfusion, ρ is density, and c_p is specific heat capacity of tissue. The conductivity changes due to electroporation and temperature variation at each point inside the tissue was calculated as [18,19]:

$$\sigma = \sigma_0 * (1 + flc2hs(E - E_{delta}, E_{range}) + \alpha * (T - T_0)) \tag{3}$$

Where σ_0 is baseline conductivity, E is electric field in the deserted point, E_{delta} is threshold electric field in electroporation, E_{range} is electric field range, α is temperature coefficient in electrical conductivity, and T and T_0 are respectively the temperature and initial temperature of tissue. Additionally, flc2hs is a smoothed Heaviside function in the COMSOL that changes from zero to one when $E - E_{delta}=0$ over the range E_{range} to ensure the convergence of the numerical solution [19]. The numerical values of the parameters used in this study are shown in Table 1 [18,19]. The simulations were conducted on a personal computer with Intel ® Core ™ i7-4770K @ 3.50 GHz processor and 16 GB of RAM.

Table 1. Parameters used in simulation

Variables	Variable values
σ_0	0.067 (S/m)
E_{delta}	580 (V/cm)
E_{range}	(120,-120) (V/cm)
α	0.015 (°C^{-1})
T_0	37 (°C)

Results

Conductivity changes in classical IRE

The conductivity changes of the eight monopolar electric pulses are presented in Figure 2. In addition, Figure 3 displays the conductivity changes of the eight bipolar electric pulses. Figure 2a illustrates the tip of the plate electrodes where eight pulses of 2500 V/cm with the frequency of 1 Hz and width of 2 ms were applied across the electrodes. Figure 2b presents the computations pertaining to between the plate electrodes. According to the results, the tissue conductivity was increased (Figure 2).

Each pulse caused an increase in tissue conductivity. The changes in conductivity occurred when the intensity of the electric field in the tissue was higher than the threshold (figures 2 and 3).

The maximum conductivity changes in the tip of and between the electrodes with monopolar pulses were 0.214 S/m and 0.1715 S/m, respectively. As can be seen in figures 2 and 3, in each case, the conductivity changes were much higher in the tip of the electrode than those in between the electrodes. The maximum conductivity changes with bipolar pulses at the tip of and between the electrodes were 0.1556 S/m and 0.1425 S/m, respectively (Figure 3). According to our results, the conductivity changes with monopolar pulses were greater than those with bipolar pulses.

Conductivity changes in IRE with high frequency

In this part, 4,000 monopolar and bipolar pulses with the frequency of 5 kHz, pulse width of 100 μs, and electric field intensity of 100-300 V/cm were used as electric pulses. Subsequently, we calculated the conductivity changes in the tip of and between the plate electrodes. Figure 4 presents the conductivity changes corresponding to a pulse with 300 V/cm. The conductivity changes at the time of the last pulse (4,000th) along with other pulses are given in Table 2.
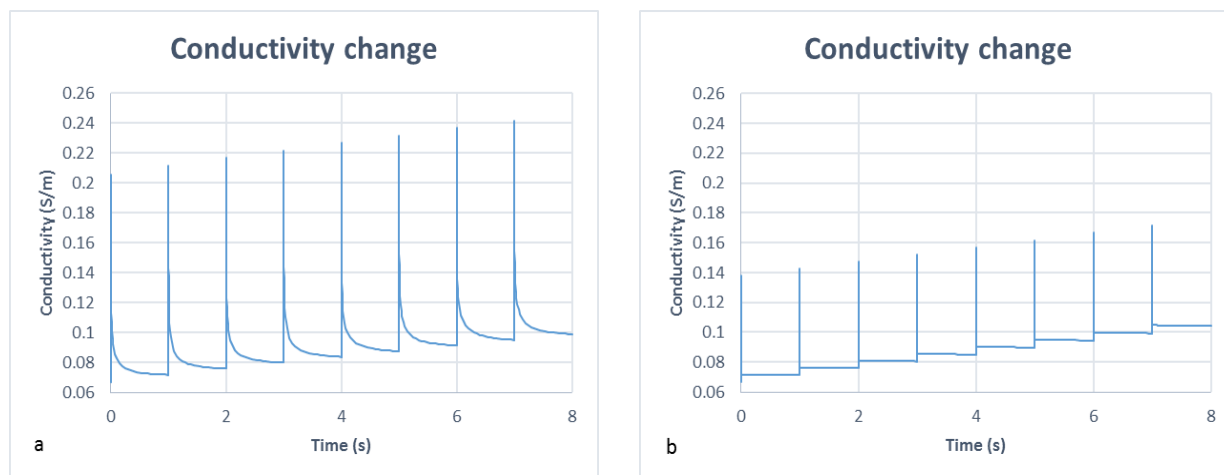

Figure 2. Conductivity changes for eight monopolar pulses with the frequency of 1 Hz, pulse width of 2 ms, and electric field intensity of 2500 V/cm a) in the tip of plate electrodes b) between the plate electrodes
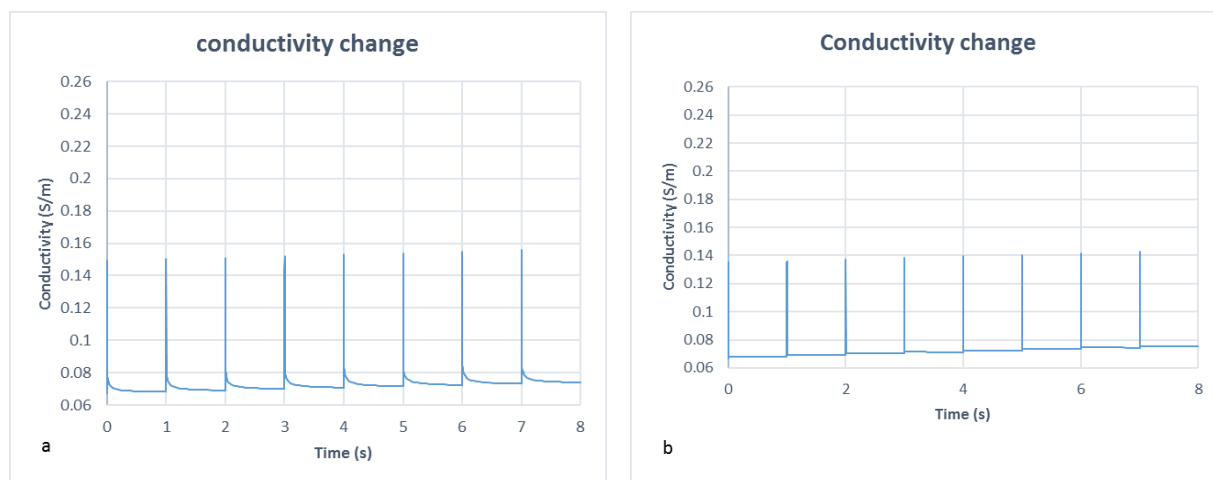
Figure 3. Conductivity changes for eight bipolar pulses with the frequency of 1 Hz, pulse width of 2 ms, and electric field intensity of 2500 V/cm a) in the tip of the plate electrodes b) between the plate electrodes
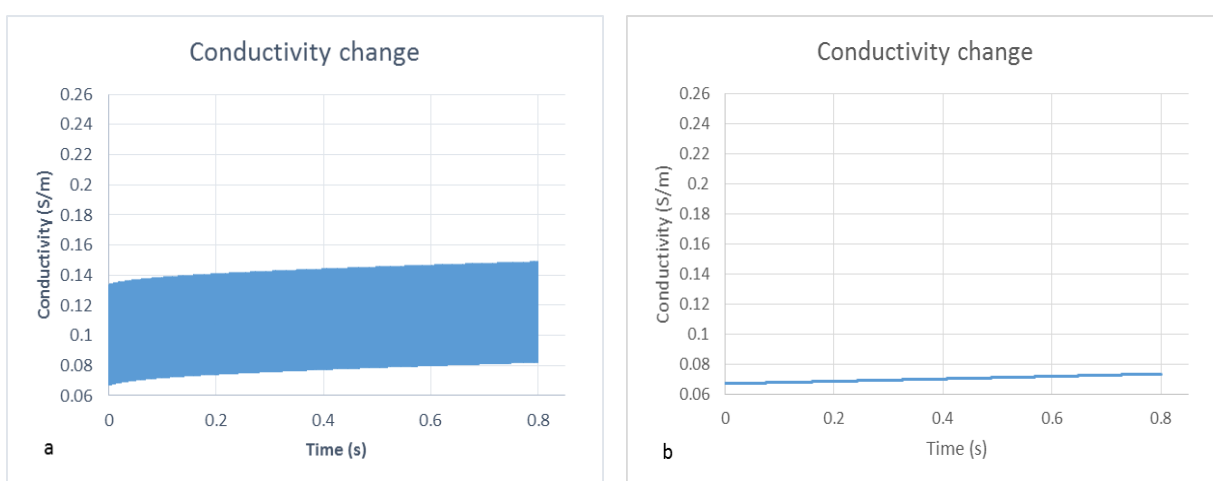

Figure 4. Conductivity changes for 4,000 monopolar pulses with the frequency of 5 kHz, pulse width of 100μs, and electric field intensity of 300 V/cm a) in the tip of the plate electrodes b) between the plate electrodes

Table 2. Conductivity change in the tip of and between the electrodes at the time of the last pulse with 4,000 monopolar and bipolar pulses with the frequency of 5 kHz, pulse width of 100μs, and electric field intensity of 100-300 V/cm

Pulses	Electric field intensity (V/cm)	Conductivity changes in the tip of the electrode (S/m)	Conductivity changes of between the electrode (S/m)
Monopolar	100	0.0685	0.0677
	150	0.0731	0.0686
	200	0.0746	0.0698
	250	0.1448	0.0715
	300	0.1491	0.0735
bipolar	100	0.0673	0.0672
	150	0.0678	0.0674
	200	0.0685	0.0677
	250	0.0694	0.0681
	300	0.0740	0.0686

Discussion

Conductivity changes in IRE with low-frequency pulse

The previous studies have investigated the electric conductivity changes during the tissue electroporation [11-14]. In the first part of our study, we performed the modeling for the HVLF IRE using monopolar and bipolar electric pulses. The findings revealed that the electrical conductivity immediately increased due to the electric field of each pulse, and then slowly returned to its original value. In agreement with the findings obtained by Miklavcic et al., we demonstrated that the conductivity changes were enhanced by increasing the pulse voltage.

Miklavcic et al. reported that conductivity increased by factors of 1.5 and 2.1 [13]. As shown in

figures 1-4 and Table 2, the conductivity changes were greater in the tip of the electrode than that in between the electrodes in all pulses due to the higher intensity of the electric field at the tip of the electrode. In 2014, Miklavcic et al. performed simulation in order to calculate the conductivity changes of the liver tissue and reported similar findings to those of our study [20]. The conductivity changes in our simulations for monopolar pulses in the tip of and between the electrodes were calculated by the factors of 3.6 and 2.55, respectively, and the changes for bipolar pulses were 2.32 and 2.12, respectively (Figure 3). The conductivity changes with monopolar pulses was greater than those induced by bipolar pulses since the monopole pulse entailed a voltage of 0-V_{max}; however, the bipolar pulses voltage varied within $(-V_{max}/2)$ to $(V_{max}/2)$.

Conductivity changes in IRE with high-frequency pulse

The HFLV electroporation is a relatively new physical tissue ablation method [21-23]. The early experiments on cell culture revealed that these protocols required substantially lower electric fields to induce cell ablation, compared to the HVLF electroporation. Therefore, we used specific electric pulses with high-frequency and low-voltage electric field for the second part of the study. The electrical conductivity immediately increased due to the electric field of the pulse, and after the pulse, the tissue conductivity slowly returned to its original value.

The conductivity changes in each pulse are given in Table 2. As indicated in this table, some of the pulses led to significant changes in conductivity. For example, in all pulses less than 250 V/cm, the conductivity changes of between the electrodes was less than 10%. Nonetheless, in the monopolar pulses with the electric field intensity of 250 and 300 V/cm, the conductivity changes were calculated by the factor of 2.1 and 2.22 at the tip of and between the electrodes, respectively. These factors were less than the changes induced by low-frequency pulses.

The conductivity changes were greater for monopolar pulses than those for the bipolar pulses. Krassowska et al. used monopolar and bipolar electric pulses for performing electroporation and recommended to use bipolar pulses due to their fewer side effects [24]. Nevertheless, based on our findings, we recommend to apply the monopolar pulses due to their fewere side effects like thermal effects and the use of low electric field intensity. Davalos et al. calculated the conductivity changes of the liver tissue with plate electrodes by the factor of 3.8. They used 99 monopolar pulses with the duration of 100 μs, frequency of 4 and 0.25 Hz, and electric field intensity of 1,000 V/cm [19]. Their findings were consistent with those of our study.

Conclusion

Electroporation relies on the electric field distribution inside the tissue, which in turn depends on the conductivity of the tissue. In in the present study, we demonstrated the occurrence of the conductivity changes during the LVHF and HVLF electroporation. However, as the findings indicated, these changes were higher for the HVLF protocol (figures 1 and 2). Therefore, in high-frequency and low-electric field pulses, ignoring the conductivity changes on the distribution of the electric field would be associated with fewer errors.

According to the literature, the IRE is achievable using the LVHF electroporation [21-23], which has significantly lower permeabilization thresholds than the HVLF electroporation. Consequently, the use of high-frequency and low-voltage produces lower temperature in the tissue and eliminates the patient's pain and muscle contraction; consequently, this protocol is recommended.

Acknowledgment

References

1. Neumann E, Schaefer-Ridder M, Wang Y, Hofschneider PH. Gene transfer into mouse lyoma cells by electroporation in high electric fields. EMBO J. 1982;1(7):841.
2. DeBruin KA, Krassowska W. Modeling electroporation in a single cell. I. Effects of fielstrength and rest potential. Biophys. J. 1999 Sep 30;77(3):1213-24. DOI: 10.1016/S0006-3495(99)76973-0.
3. Adeyanju O, Al-Angari H, Sahakian A. The optimization of needle electrode number and placement for IRE of hepatocellular carcinoma. Radiol Oncol. 2012 Jun 1;46(2):126-35. DOI: 10.2478/v10019-012-0026-y.
4. Miklavčič D, Beravs K, Šemrov D, Čemažar M, Demšar F, Serša G. The importance of electric field distribution for effective in vivo electroporation of tissues. Biophys. J. 1998 May 31;74(5):2152-8. DOI: 10.1016/S0006-3495(98)77924-X.
5. Lu DS, Kee ST, Lee EW. IRE: ready for prime time? Tech Vasc Interv Radiol. 2013;16(4):277-86. DOI: 10.1053/j.tvir.2013.08.010.
6. Mir LM. Therapeutic perspectives of in vivo cell electropermeabilization. Bioelectrochemistry. 2001 Jan 1;53(1):1-0. DOI: 10.1016/S0302-4598(00)00112-4.
7. Arena CB, Sano MB, Rossmeisl JH, Caldwell JL, Garcia PA, Rylander MN, et al. High-frequency IRE (H-FIRE) for non-thermal ablation without muscle contraction. Biomed Eng Online. 2011;10(1):102. DOI: 10.1186/1475-925X-10-102.

8. Reilly JP, Freeman VT, Larkin WD. Sensory effects of transient electrical stimulation-evaluation with a neuroelectric model. IEEE Trans. Biomed. Eng. 1985 Dec(12):1001-11. DOI: 10.1109/TBME.1985.325509.

9. Miklavcic D, Pucihar G, Pavlovec M, Ribaric S, Mali M, Macek-Lebar A, et al. The effect of high frequency electric pulses on muscle contractions and antitumor efficiency in vivo for a potential use in clinical electrochemotherapy. Bioelectrochemistry. 2005;65(2):121-8. DOI: 10.1016/j.bioelechem.2004.07.004.

10. Corovic S, Zupanic A, Miklavcic D. Numerical modeling and optimization of electric field distribution in subcutaneous tumor treated with electrochemotherapy using needle electrodes. IEEE Trans. Plasma Sci. 2008 Aug;36(4):1665-72. DOI: 10.1109/TPS.2008.2000996.

11. Dunki-Jacobs EM, Philips P, Martin RC. Evaluation of resistance as a measure of successful tumor ablation during IRE of the pancreas. J. Am. Coll. Surg. 2014 Feb 28;218(2):179-87. DOI: 10.1016/j.jamcollsurg.2013.10.013.

12. Moisescu MG, Radu M, Kovacs E, Mir LM, Savopol T. Changes of cell electrical parameters induced by electroporation. A dielectrophoresis study. Biochim. Biophys. Acta. 2013 Feb 28;1828(2):365-72. DOI: 10.1016/j.bbamem.2012.08.030.

13. Kranjc M, Bajd F, Serša I, Miklavčič D. Magnetic resonance electrical impedance tomography for measuring electrical conductivity during electroporation. Physiol Meas. 2014 May 20;35(6):985.

14. Ivorra A, Rubinsky B. In vivo electrical impedance measurements during and after electroporation of rat liver. Bioelectrochemistry. 2007 May 31;70(2):287-95. DOI: 10.1016/j.bioelechem.2006.10.005.

15. Pavlin M, Kandušer M, Reberšek M, Pucihar G, Hart FX, Magjarevićcacute R, et al. Effect of cell electroporation on the conductivity of a cell suspension. Biophys. J. 2005 Jun 30;88(6):4378-90. DOI: 10.1529/biophysj.104.048975.

16. Cukjati D, Batiuskaite D, André F, Miklavčič D, Mir LM. Real time electroporation control for accurate and safe in vivo non-viral gene therapy. Bioelectrochemistry. 2007 May 31;70(2):501-7. DOI: 10.1016/j.bioelechem.2006.11.001.

17. Glahder J, Norrild B, Persson MB, Persson BR. Transfection of HeLa-cells with pEGFP plasmid by impedance power-assisted electroporation. Biotechnol. Bioeng. 2005 Nov 5;92(3):267-76. DOI: 10.1002/bit.20426.

18. Garcia PA, Rossmeisl Jr JH, Neal II RE, Ellis TL, Olson JD, Henao-Guerrero N, et al. Intracranial nonthermal IRE: in vivo analysis. J. Membr. Biol. 2010 Jul 1;236(1):127-36. DOI: 10.1007/s00s232-010-9284-z.

19. Sano MB, Neal RE, Garcia PA, Gerber D, Robertson J, Davalos RV. Towards the creation of decellularized organ constructs using IRE and active mechanical perfusion. Biomed Eng Online. 2010 Dec 10;9(1):83. DOI: 10.1186/1475-925X-9-83.

20. Garcia PA, Davalos RV, Miklavcic D. A numerical investigation of the electric and thermal cell kill distributions in electroporation-based therapies in tissue. PloS one. 2014 Aug 12;9(8):e103083. DOI: 10.1371/journal.pone.0103083.

21. Shankayi Z, Firoozabadi SM, Hassan ZS. Optimization of Electric Pulse Amplitude and Frequency In Vitro for Low Voltage and High Frequency Electrochemotherapy. The Journal of membrane biology. 2014 Feb 1;247(2):147-54. DOI: 10.1007/s00232-013-9617-9.

22. Shankayi Z, Saraf Hassan Z. Comparison of low voltage amplitude electrochemotherapy with 1 Hz and 5 kHz frequency in volume reduction of mouse mammary tumor in Balb/c Mice. Koomesh. 2012 Jun 15;13(4):486-90.

23. Shankayi Z, Firoozabadi SM, Saraf HZ. The Endothelial Permeability Increased by Low Voltage and High Frequency Electroporation. Journal of biomedical physics & engineering. 2013 Sep;3(3):87.

24. Bilska AO, DeBruin KA, Krassowska W. Theoretical modeling of the effects of shock duration, frequency, and strength on the degree of electroporation. Bioelectrochemistry. 2000 Jun 30;51(2):133-43. DOI: 10.1016/S0302-4598(00)00066-0.